Flexible calibration technique for fringe-projection-based three-dimensional imaging

Minh Vo,[1] Zhaoyang Wang,[2,*] Thang Hoang,[1,2] and Dung Nguyen[1]

[1]*Department of Electrical Engineering, The Catholic University of America, Washington, D.C. 20064, USA*

[2]*Department of Mechanical Engineering, The Catholic University of America, Washington, D.C. 20064, USA*

**Corresponding author: wangz@cua.edu*

Received July 15, 2010; revised September 2, 2010; accepted September 3, 2010;
posted September 9, 2010 (Doc. ID 131725); published September 21, 2010

Fringe projection profilometry (FPP) has evolved dramatically, with many highly demanded features for three-dimensional (3D) imaging, such as high accuracy, easy implementation, and capability of measuring multiple objects with complex shapes. A vital component for an FPP-based 3D imaging system is the calibration process. The existing calibration methods lack the ability to be flexibly compatible with various scales of the field of imaging. In this Letter, a technique to cope with this issue is presented; it employs a checkerboard along with practical considerations to ensure reliable and accurate calibration. The validity and practicality of the technique are verified by experiments.

OCIS codes: 110.6880, 120.2830, 120.6660, 150.6910.

Fringe projection profilometry (FPP) is one of the most prevalent methods for acquiring three-dimensional (3D) images of objects because of its numerous advantages, such as low cost, easy implementation, full-field imaging, and high accuracy. A notable challenge faced by the technique is the flexibility in the scale of the field of view.

A typical FPP-based 3D imaging system comprises a camera, a projector, and a computer. The camera and the projector can usually be positioned arbitrarily to form a generalized setup. To perform high-quality 3D imaging, proper calibration is essential for the FPP technique. At present, there are two common calibration approaches. The first one treats the projector as a reversed camera [1] and uses a camera calibration method to calibrate both the camera and the projector. With projection fringes as a tool to establish the correspondence, 3D coordinates of points can be determined by mapping the locations of points in the camera with those in the projector; thus, the imaging mechanism returns to the traditional stereovision technique. However, a well-known drawback of this approach is that the calibration of a projector is complicated and error prone [2].

The second calibration approach is based on a governing equation that relates the height or depth information of the object surface to the phase map of the projection fringes at each point [3,4], and it employs a number of gage blocks of different heights to calibrate the system. This method is easy to implement and can yield very accurate results. Nevertheless, the challenge lies in manufacturing high precision gage blocks for various applications, because the block sizes have to be changed according to the field of imaging, which may range from very small to very large scales. The difficulty and high cost of manufacturing a larger number of precise gage blocks make the calibration technique impractical.

This Letter proposes a calibration approach to cope with the limitations of the existing techniques while providing accurate 3D imaging. The approach takes advantage of the flexibility of the calibration checkerboard from the aforementioned first method and the advance of the governing equation from the second method. The proposed method does not require calibration of the projector, and the entire calibration procedure is completed by a process similar to the commonly used camera calibration [5], except that fringes will be projected onto the checkerboard. The technique is elaborated below.

In 3D imaging, the primary task is to obtain the out-of-reference-plane height or depth information of an object or object system. For a generalized FPP system with an arbitrary arrangement of components, the governing equation of the 3D height determination is [6,7]

$$\begin{aligned} z &= f_c/f_d \\ f_c &= 1 + c_1\phi + (c_2 + c_3\phi)i + (c_4 + c_5\phi)j \\ &\quad + (c_6 + c_7\phi)i^2 + (c_8 + c_9\phi)j^2, \\ f_d &= d_0 + d_1\phi + (d_2 + d_3\phi)i + (d_4 + d_5\phi)j \\ &\quad + (d_6 + d_7\phi)i^2 + (d_8 + d_9\phi)j^2, \end{aligned} \tag{1}$$

where z is the out-of-reference-plane height or depth at pixel (i, j), ϕ is the phase of the projection fringe at the same pixel, and c_1–c_9 and d_0–d_9 are constant coefficients associated with the geometrical and other system parameters. In practice, the distribution of phase ϕ is usually determined by using a multifrequency phase-shifting technique, which is capable of providing full-field unwrapped phase in a direct and ultrafast manner for 3D imaging of multiple objects with complex shapes [7].

To calibrate the FPP system for 3D imaging at different scales, a number of checkerboards of various sizes are employed to determine the 19 coefficients c_1–c_9 and d_0–d_9. On each board, there are at least tens of squares arranged in alternating white and black. In the experiments carried out in this Letter, each checkerboard consists of 130 squares (10 rows and 13 columns) of the same size, and the square sizes range from 2.44 mm to 50.80 mm for these checkerboards. The calibration involves obtaining the 3D coordinates of every point of interest on the checkerboard surface at a number of positions. The 3D coordinates serve as gages to determine the 19 coefficients using a least-squares approach. Here, the multiple positions and least-squares algorithm help to

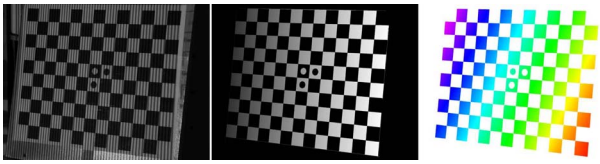

Fig. 1. (Color online) Representative images of system calibration: checkerboard with projection fringes, unwrapped phase map, and out-of-reference-plane height map.

ensure high accuracy and fidelity. The technical details are described as follows.

The proposed calibration technique requires capturing a series of images of the checkerboard at different positions with phase-shifted fringes projected on the board. For each position, a clear checkerboard image can be obtained by adding up the captured fringe images. The clear checkerboard images at all the positions are subsequently used to find the intrinsic and extrinsic parameters of the camera [5,8]. The intrinsic parameters are useful for correcting the distortion of the camera lens, and the extrinsic parameters (i.e., the transformation matrix) are needed for detecting the 3D coordinates of each point on the checkerboard. Defining the points in the camera and world coordinate system as $\{x_c, y_c, z_c\}^T$ and $\{x_w, y_w, z_w\}^T$, respectively, and setting z_w to 0 without loss of generality, a simple relation between the camera and world coordinate systems is expressed as

$$\begin{Bmatrix} x_c \\ y_c \\ z_c \end{Bmatrix} = \begin{bmatrix} R_{11} & R_{12} & T_1 \\ R_{21} & R_{22} & T_2 \\ R_{31} & R_{32} & T_3 \end{bmatrix} \begin{Bmatrix} x_w \\ y_w \\ 1 \end{Bmatrix}, \tag{2}$$

where R and T denote the rotation and translation elements of the transformation matrix, respectively. Since x_w and y_w for each corner of the checkerboard are precisely known, Eq. (2) allows the locations of all the board corners in the camera coordinate system to be found. Letting the checkerboard surface at the first position be the reference plane, the plane can be described as

$$Ax_c^r + By_c^r + Cz_c^r + 1 = 0, \tag{3}$$

where A, B, and C are the planar parameters, and $\{x_c^r, y_c^r, z_c^r\}^T$ indicates an arbitrary point on the reference checkerboard plane. Although only three corner points are needed to form a plane, using all the corners to solve for the three planar parameters with a least-squares algorithm helps to enhance the accuracy.

Once A, B, and C in Eq. (3) are finalized, the height of each corner on the checkerboard at any other position $\{x_c, y_c, z_c\}^T$, with respect to the reference plane, can be expressed as

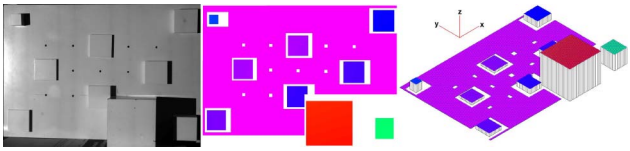

Fig. 2. (Color online) 3D imaging results of a plate with gage blocks.

Table 1. Actual and Measured Heights of Gage Blocks[a]

Block No.	Actual	Measured	Error
1	25.40	25.16	−0.24
2	19.05	19.23	0.18
3	6.35	6.27	−0.08
4	6.35	6.28	−0.07
5	12.70	12.59	−0.11
6	15.88	15.71	−0.17
7	9.53	9.63	0.10
8	101.60	101.42	−0.18
9	50.80	50.95	0.15

[a]Unit: millimeters.

$$z^b = \frac{Ax_c + By_c + Cz_c + 1}{\sqrt{A^2 + B^2 + C^2}}. \tag{4}$$

A bilinear interpolation process is performed to obtain the out-of-reference-plane heights of the points within the white regions on the checkerboard. It is noted that every point in the black regions is excluded because the phase ϕ there contains high noise. Figure 1 shows a representative image of the checkerboard with fringes projected onto it, the corresponding unwrapped phase map, and the out-of-reference-plane height map.

After the unwrapped phase ϕ and height z^b distributions of the points at all the checkerboard positions are obtained, the system calibration can be carried out to determine the coefficients c_1–c_9 and d_0–d_9 through minimizing a nonlinear least-squares error defined as

$$S = \sum_{k=1}^{m} \left(\frac{f_c}{f_d} - z_k^b \right)^2, \tag{5}$$

where z_k^b denotes the absolute out-of-reference-plane heights of the points on the checkerboards at various positions, k is the ordinal number of each point, and m is the total number of points valid for calibration. The least-squares criterion requires

$$\frac{\partial S}{\partial c_p} = 0, \quad p = 1, 2, ..., 9, \quad \frac{\partial S}{\partial d_q} = 0, \quad q = 0, 1, ..., 9. \tag{6}$$

The coefficients c_1–c_9 and d_0–d_9 can be determined by using Levenberg–Marquardt algorithm, where an initial guess can be provided by minimizing a linear least-squares error in the form of $S = \sum_{k=1}^{m} (f_c - f_d z_k^b)^2$. It is noted that at least three different positions of the checkerboard must be utilized to correctly determine the coefficients because of the complexity of the governing equation and the simplicity of each board-plane

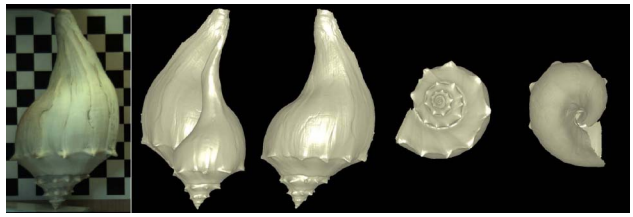

Fig. 3. (Color online) Conch shell and its 3D images from four views.

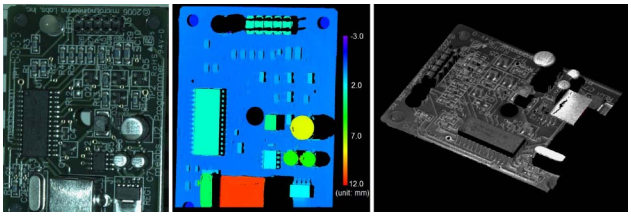

Fig. 4. (Color online) Printed circuit board, the 2D height map, and the 3D rendered height map.

function. It is also important to point out that, although using a relatively large number of positions (e.g., over 50 positions) can help enhance the accuracy [8], experiments reveal that using 10–20 positions is normally sufficient in practice. In this Letter, 20 positions are adopted, and they cover the volume of the imaging field to assure good accuracy over the entire field.

To demonstrate the validity of the proposed technique, a few experiments have been conducted at various scales of the field of view. The first experiment aimed to test the imaging accuracy, where a flat plate of 457.2 mm × 304.8 mm with nine highly precise gage blocks and a checkerboard with a square size of 20.32 mm were selected as the target of interest and calibration board, respectively. Figure 2 shows the testing plate together with its experimentally obtained 2D and 3D plots. Table 1 indicates that the maximum error over the entire field of imaging is 0.24 mm, which yields a relative accuracy (defined as the ratio of out-of-plane measurement accuracy to the in-plane dimension) of 0.052%. This confirms the validity and reliability of the technique. It may be helpful to clarify that lens-distortion correction was not applied to the calibration and imaging, because the governing equation, Eq. (1), was designed to take into account the lens-distortion effect.

The other three experiments were intended to verify the flexibility of the proposed technique for 3D imaging at various scales. Figure 3 illustrates the full 360° 3D imaging result of a conch shell of 221 mm length obtained by combining the 3D images captured from multiple views. Visual inspection shows that the full 360° image has a very good match with the actual object, and the surface structure can be clearly seen.

The next experiment was conducted to confirm the ability of 3D imaging at small scales, where a small calibration checkerboard with a square size of 2.44 mm was employed. An optical lens was added to the system to focus the projection fringes into a small region. Figure 4 shows the imaging result of a printed circuit board

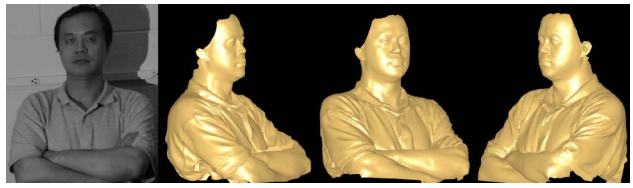

Fig. 5. (Color online) Human body and the 3D images from three views.

of 44.0 mm width with many small components on it. It can be seen that, except for the shadow and shiny regions, the result indicates a good imaging accuracy.

The last experiment was implemented to show the performance of the technique on 3D shape measurements at relatively large scales, where a large calibration checkerboard with a square size of 50.80 mm was utilized. Figure 5 shows the 3D shape measurement result of a human body. This and the previous experimental results evidently demonstrate that the proposed technique is capable of accurately providing 3D imaging or measuring 3D shapes of objects at various scales as long as the size of the calibration board matches the field of imaging.

In conclusion, an approach to calibrating an FPP-based 3D imaging system is introduced, and its validity and practicality have been verified by experiments. Because only one checkerboard of appropriate size is required for each imaging scenario, and the checkerboard pattern can be printed out by a regular printer, the calibration technique is remarkably flexible and convenient to use. In addition to checker patterns, the calibration board may use circle or ring patterns.

The work is supported by the National Science Foundation (NSF) (grant CMMI-0825806) and the National Collegiate Inventors and Innovators Alliance (grant 5205-07).

References

1. Z. Li, Y. Shi, C. Wang, and Y. Wang, Opt. Eng. **47**, 053604 (2008).
2. X. Zhang and L. Zhu, Opt. Eng. **48**, 117208 (2009).
3. H. Du and Z. Wang, Opt. Lett. **32**, 2438 (2007).
4. S. Cui and Z. Zhu, Opt. Express **17**, 20735 (2009).
5. Z. Zhang, IEEE Trans. Pattern Anal. Machine Intell. **22**, 1330 (2000).
6. L. Huang, P. Chua, and A. Asundi, Appl. Opt. **49**, 1539 (2010).
7. Z. Wang, D. Nguyen, and J. Barnes, Opt. Lasers Eng. **48**, 218 (2010).
8. D. Douxchamps and K. Chihara, IEEE Trans. Pattern Anal. Machine Intell. **31**, 376 (2009).